

1.7 Gbit/in.² gray-scale continuous-phase-change femtosecond image storage

Q. Wang,^{1,2,a)} J. Maddock,¹ E. T. F. Rogers,¹ T. Roy,¹ C. Craig,¹ K. F. Macdonald,¹ D. W. Hewak,¹ and N. I. Zheludev^{1,3}

¹*Optoelectronics Research Centre and Centre for Photonic Metamaterials, University of Southampton, Highfield, Southampton, SO17 1BJ, United Kingdom*

²*Institute of Materials Research and Engineering, 3 Research Link, Singapore 117602, Singapore*

³*Centre for Disruptive Photonic Technologies, Nanyang Technological University, Singapore 637371, Singapore*

(Received 20 January 2014; accepted 14 March 2014; published online 25 March 2014)

We demonstrate high-density, multi-level crystallization of a Ge₂Sb₂Te₅ thin film using tightly focused femtosecond laser pulses. The submicron spots with 8 distinct data storage states are written on a 1.08 μm square grid. The significant change in reflectivity of every specific state of crystallized spot allows easy optical reading and identification. As a demonstration, two gray-scale images are written into the storage medium. Our results open up potential applications in ultra-fast two-dimensional parallel cognitive computing and holography. © 2014 AIP Publishing LLC. [<http://dx.doi.org/10.1063/1.4869575>]

Chalcogenide glasses were originally presented by Ovshinsky as a promising candidate for non-volatile data storage, through switching between amorphous and crystalline phase states.¹ Typical chalcogenides, such as Germanium-Antimony-Telluride (GeSbTe), exhibit large changes of optical reflectivity, electronic conductivity, and thermal conductivity between amorphous and crystalline phases, and are easily changed between these states using optical, electrical, or thermal energy.² These remarkable properties make chalcogenide glass an excellent rewritable optical data-recording medium.³ GeSbTe can also form intermediate states, where the material contains regions in both the amorphous and crystalline states, which are attractive for applications in solid-state storage devices.^{4–7} Recently, attention has focused on cumulative switching of GeSbTe films induced by ultrafast lasers, where the repeatable energy dose and rapid heat diffusion allow control of the crystallization process.^{8–11} By repeatedly exposing the same area of a GeSbTe film to femtosecond laser pulses, a continuous change of reflectivity was achieved.^{12,13} This partial crystallization allows multi-level optical data storage, analogous to electrical multi-level storage.¹⁰

Conventionally, high-density optical-data-storage efforts work to minimize the footprint of the recorded bits. An alternative is to increase the number of bits stored in each recording units. In this paper, we demonstrate high-density image storage by writing multi-level scale data on a chalcogenide film. Each gray-scale level is achieved by delivering a specific amount of pulse energy to the targeted point on the GeSbTe film, where the well-defined spot shape, the submicron-sized spot area and the large change in reflectivity available are the crucial factors in accurate writing. Additionally, recent studies demonstrate that a specifically designed film-substrate system allows reversible phase switching using a single femtosecond laser pulse,¹⁴ but in commercial optical data storage the typical time-scale for

data recording and erasing is several hundred nanoseconds. Therefore, the use of the femtosecond lasers for optical data storage could dramatically reduce the laser-beam exposure time for data storage and erasure.

We use Ge₂Sb₂Te₅ (GST) as our phase-change material which is a semiconductor chalcogenide alloy with a crystallization temperature T_c of about 160 °C and a melting temperature T_m of about 600 °C.¹⁴ The film will be crystallized if it is heated above its crystallization temperature, but without reaching the melting temperature. In conventional binary optical data storage (rewritable optical discs and phase-change random-access memory), a single excitation event completely switches the phase state. In contrast, we locally heat the film using focused femtosecond laser pulses, but we control the pulse energy so that we bring the film to around T_c ; hence it only partially crystallises. The degree of crystallization is probed by measuring the optical reflectivity of the submicron switched area.

Figure 1 shows a schematic diagram of the experimental setup. The laser source is a titanium-sapphire femtosecond laser (Coherent Chameleon Vision S) generating 80 MHz train of 85 fs pulses at 730 nm wavelength. We use an electro-optical modulator (Conoptics Corp.) to select single pulses. The output from the pulse picker is then expanded through a telescope system and incident on a spatial light modulator (SLM), for control of the beam scanning and focusing on the sample surface. The modulated beam is imaged by a 4f telescope system onto the back aperture of an objective lens (Nikon UL Plan Fluor 50×, 0.8 numerical aperture), which focuses the light on the sample surface. The phase-change medium (Figure 1 inset) is made by sputtering a film of GST sandwiched between two ZnS:SiO₂ layers to aid thermal diffusion and prevent oxidation, all 50 nm thin and supported on a 170 μm thick silica substrate. The changes in reflectivity of crystallized GST film are detected by using a CCD camera through a 50 × (0.7 numerical aperture) objective, under incoherent monochromatic (633 nm) illumination. A spot on the GST film is written by using

^{a)}Q.WANG@soto.ac.uk

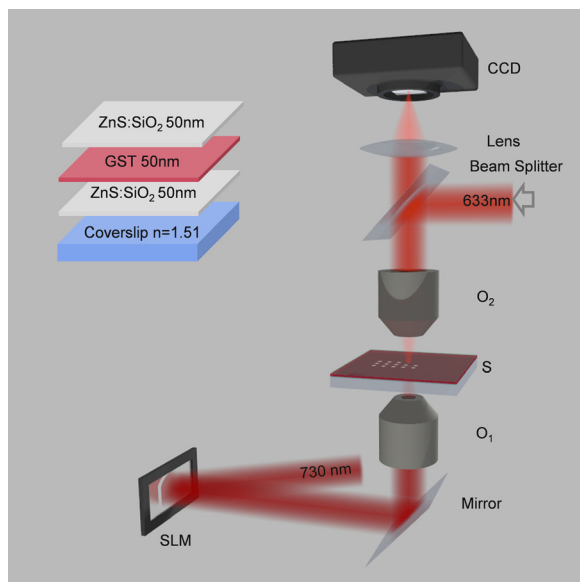


FIG. 1. Experimental setup for gray-scale femtosecond image storage. Monochromatic light from a Ti-sapphire femtosecond laser is incident on a SLM, which is focused on the sample (S) through a $50\times$, 0.8 numerical aperture (NA) objective (O_1). Depending on incident pulse energy crystallized spots are written on the GST film which are imaged in reflection under 633 nm illumination through a $50\times$, 0.7 NA objective (O_2). The inset shows the three-layer structure of GST sample with coverslip substrate.

successive low-energy pulses to initiate nucleation and crystal growth. The number of pulses is varied to achieve different reflectivity levels. The separation between pulses is set to $1\ \mu\text{s}$, which is sufficient to ensure the system thermally relaxes between pulses and hence the crystallization level of the GST film depends only on the total number of incident pulses. After each pulse, a microscope image of the film is recorded to measure the relative change of reflectivity. For imaging the crystallized spot, a mechanical shutter is used to block any leakage through the electro-optic modulator.

Figure 2(a) shows three typical characteristic curves illustrating the change in optical reflectivity of the partial crystallization GST mark under pulsed illumination. The change in reflectivity is calculated using the formula $(R_c - R_a)/R_a$, where R_c is the peak reflectivity of the spot, and R_a is the average reflectivity of the amorphous GST film over the rectangular area around the GST mark (inset to Fig. 2(a)). The results clearly show the energy accumulation and partial crystallization of GST. With 0.21 nJ pulse excitation, there is no detectable change in reflectivity until after 45 pulses, where the crystallization threshold was reached and the reflectivity begins to change. With 0.28 nJ pulse energy, the reflectivity of GST mark increases gradually with the number of pulses. While with the 0.36 nJ pulse energy, the reflectivity of the GST film increases quickly with the number of pulses and the material was switched to a high reflectivity crystalline state. Since the mapping of reflectivity of the partially crystallized spots is based on the readout value of a single pixel in the centre of the spot, the noise in the curve is mainly due to CCD read noise.

Since crystallization of a GST thin film is strongly dependent on the pulse energy applied, in the following experiments, the pulse energy is adjusted so that the first pulse incident on the GST film results in a 2.5% change in

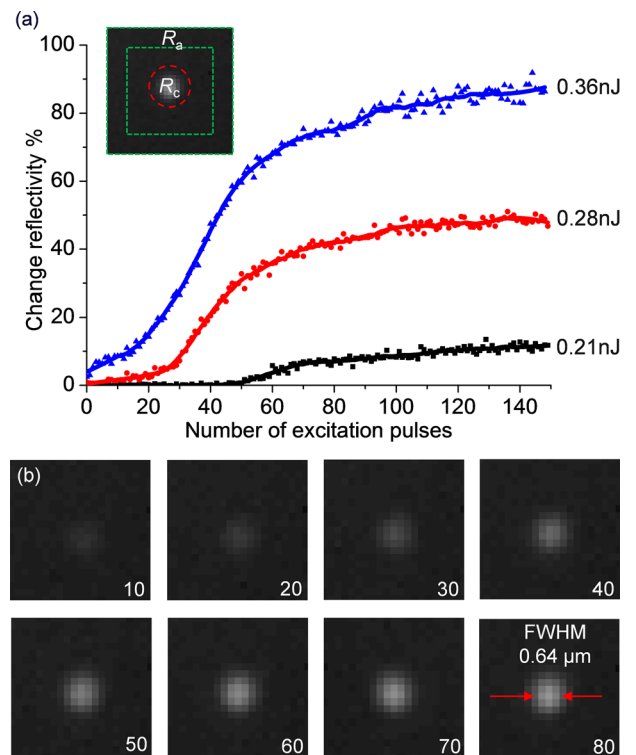


FIG. 2. An experimentally measured change in optical reflectivity $((R_c - R_a)/R_a)$ of the GST sample as a function of the pulse number of 85 fs femtosecond duration with different pulse energy applied, where R_c is the peak reflectivity of the spot, and R_a is the average reflectivity of the amorphous GST film over the rectangular area around the GST mark. (a) Solid lines are smoothed curves (Savitzky-Golay method) of the according experimental data, and the inset demonstrates the R_a and R_c area for calculation. (b) Images of the stages of crystallization of GST mark after each 10 pulses excitations of 0.36 nJ pulse energy. The mark size is typically about $0.64\ \mu\text{m}$ in full width half maximum.

reflectivity. As the number of pulses increases, the GST film undergoes first nucleation and then growth of crystallites, as shown in Fig. 2(a) (blue line). The change of reflectivity reaches 81% after 100 pulses. After that, the GST film reaches a fully crystallized state where the shape and reflectivity of spot does not change significantly. This large reflectivity variation lets us use intermediate reflectivity levels to store multiple bits in each phase-switched domain.

We use a tilted phase mask on SLM scan the focus across the sample surface, writing a different gray level at each point. As shown in Fig. 3(a), an 8-level spiral plate pattern was written on the GST film, where each level is written with a specific number of pulses—calculated from the non-linear curve in the Fig. 2(a)—to write 8 gray-levels with increasing reflectivity. Fig. 3(b) shows the average of change in reflectivity in each segment of the pattern. The average reflectivity of GST mark is linearly increasing, as expected. With more accurate control of the pulse energy, and optimization of the read out system, it will be possible to reduce the variation between spots and hence increase the number of levels reliable to be written and read.

To demonstrate the practicality of complex imaging, a portrait of a little girl was written into the GST film with the same way (Fig. 3(d)). The original photo (Fig. 3(c)) was converted to an 8-level gray-scale image with 40×61 pixels, and the computer triggered the required number of pulses

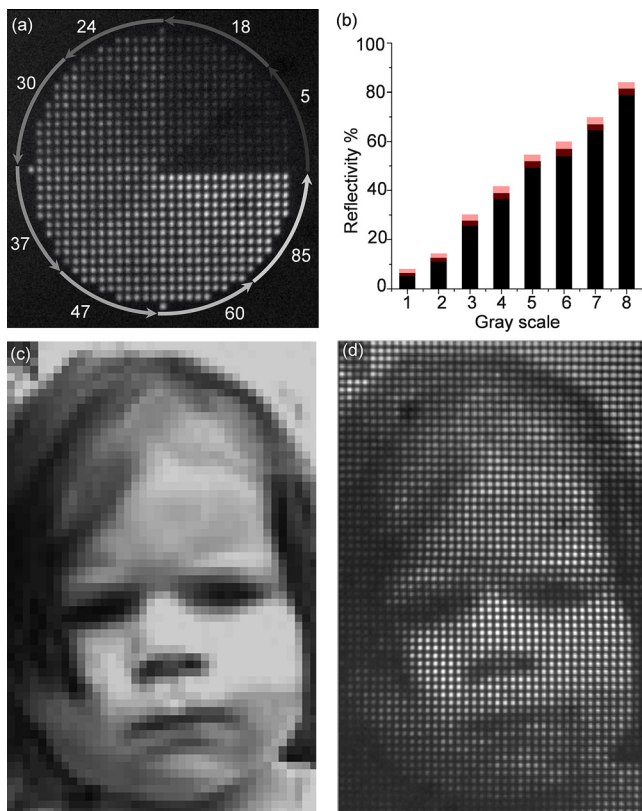


FIG. 3. Gray-scale images with GST material. (a) A spiral plate pattern of showing 8 levels of gray-scale (total diameter $34\ \mu\text{m}$). Arrows show the direction of the increasing number (from 5 to 85) of pulses incident on the GST film. (b) The average change in reflectivity of each level with standard deviation bar. (c) The original 40×61 pixels gray-scale portrait of a little girl. (d) A $43\ \mu\text{m} \times 66\ \mu\text{m}$ gray-scale portrait of a little girl.

onto each point on the sample, using the SLM to control the beam scanning. As the gray-levels are directly coded into the film, it can easily read as a single microscope image. Any bit pattern stored in multi-level GST film can be thought of equivalent to such a gray-scale image.

In a multi-level storage system, the achievable data storage density is determined by the number of levels available, as well as the spacing of the stored bits. With 8 levels (equivalent to 3 bits/mark) and a $1.08\ \mu\text{m}$ square grid, we have demonstrated a storage density of $1.7\ \text{Gbit}/\text{in}^2$ using $730\ \text{nm}$ wavelength writing pulses. To increase the storage capacity further, it is possible to reduce the spot pitch by using a shorter wavelength and higher numerical aperture, as well as increasing the accuracy of reading and writing to allow a greater number of levels. Even greater improvements in optical storage density may be possible using super-oscillatory focusing systems.^{15–17} We argue that operating at the wavelength of $473\ \text{nm}$ and using super-oscillatory solid-immersion needle lens focusing into a $\lambda/10$ hotspot,¹⁸ it could well be possible to achieve storage density of up to $186\ \text{Gbit}/\text{in}^2$. As an alternative to gray-scale image writing, two impressive techniques were recently proposed for color image writing at the nanoscale.^{19,20} From a data-storage perspective, these techniques give an extra spectral degree of freedom that increases storage density, but would require multiple read wavelengths and it is not clear if this gives a greater increases in density than our 8-level grayscale system. More importantly, they are both write-once techniques,

whereas the GST based writing proposed here is potentially rewritable. Writing of our grayscale images also uses only standard optical systems, without the need for costly electron beam lithography or focused ion beam milling.

In conclusion, we have demonstrated multi-level data storage and gray-scale image writing in a thin GST film using femtosecond laser. Our results have the potential to dramatically increase the optical data storage density in phase-change materials. Furthermore, the proposed femtosecond multi-level data storage opens up potential applications in ultra-fast two-dimensional parallel data processing, such as image encoding/decoding, rewritable amplitude masks, or holography. Additionally, the cumulative effects in controllable phase transition of GST films give the interesting prospect of realizing cognitive image processing.²¹

The work is partially supported by the Advanced Optics in Engineering Programme from the Agency for Science, Technology and Research (A*STAR) of Singapore with Grant No. 122-360-0009, the UK Engineering and Physical Sciences Research Council with Grant Nos. EP/F040644/1 and EP/G060363/1, the Royal Society of London. Q. Wang acknowledges the fellowship support from the Agency for Science, Technology and Research, Singapore. E. Rogers acknowledges support from the University of Southampton Enterprise Fund.

¹S. R. Ovshinsky, *Phys. Rev. Lett.* **21**, 1450 (1968).

²M. H. R. Lankhorst, B. W. S. M. M. Ketelaars, and R. A. M. Wolters, *Nature Mater.* **4**, 347 (2005).

³M. Mansuripur, *Crit. Technol. Future Comput.* **4109**, 162–176 (2000).

⁴J. H. Coombs, A. P. J. M. Jongenelis, W. v. Es-Spiekman, and B. A. J. Jacobs, *J. Appl. Phys.* **78**, 4906 (1995).

⁵B. S. Lee, G. W. Burr, R. M. Shelby, S. Raouf, C. T. Rettner, S. N. Bogle, K. Darmawikarta, S. G. Bishop, and J. R. Abelson, *Science* **326**, 980–984 (2009).

⁶L. P. Shi, T. C. Chong, P. K. Tan, X. S. Miao, Y. M. Huang, and R. Zhao, *Jpn. J. Appl. Phys., Part 1* **38**, 1645–1648 (1999).

⁷M. Xu, S.-J. Wei, S. Wu, J. L. F. Pei, S.-Y. Wang, L.-Y. Chen, and Y. Jia, *J. Korean Phys. Soc.* **53**, 2265–2269 (2008).

⁸J. Siegel, W. Gawelda, D. Puerto, C. Dorronsoro, J. Solis, C. N. Afonso, J. C. G. de Sande, R. Bez, A. Pirovano, and C. Wiemer, *J. Appl. Phys.* **103**, 023516 (2008).

⁹W. Zhu, Y. Lu, S. Li, Z. Song, and T. Lai, *Opt. Express* **20**, 18585–18590 (2012).

¹⁰S. R. Ovshinsky, *Jpn. J. Appl. Phys., Part 1* **43**, 4695–4699 (2004).

¹¹J. Bonse, G. Bachelier, J. Siegel, and J. Solis, *Phys. Rev. B* **74**, 134106 (2006).

¹²C. D. Wright, Y. Liu, K. I. Kohary, M. M. Aziz, and R. J. Hicken, *Adv. Mater.* **23**, 3408 (2011).

¹³Y. Liu, M. M. Aziz, A. Shalini, C. D. Wright, and R. J. Hicken, *J. Appl. Phys.* **112**, 123526 (2012).

¹⁴B. Gholipour, J. Zhang, K. F. MacDonald, D. W. Hewak, and N. I. Zheludev, *Adv. Mater.* **25**, 3050–3054 (2013).

¹⁵E. T. F. Rogers and N. I. Zheludev, *J. Opt.* **15**, 094008 (2013).

¹⁶J. r. Baumgartl, S. Kosmeier, M. Mazilu, E. T. F. Rogers, N. I. Zheludev, and K. Dholakia, *Appl. Phys. Lett.* **98**, 181109 (2011).

¹⁷E. T. F. Rogers, S. Savo, J. Lindberg, T. Roy, M. R. Dennis, and N. I. Zheludev, *Appl. Phys. Lett.* **102**, 031108 (2013).

¹⁸G. Yuan, E. T. F. Rogers, T. Roy, B. Lafferty, M. Mooney, Z. X. Shen, and N. I. Zheludev, *Conference on Lasers and Electro-Optics (CLEO) 2013, San Jose, United States, 09–14 June 2013*, p. QM1B.8.

¹⁹J. Zhang, J. Y. Ou, N. Papisimakis, Y. Chen, K. F. Macdonald, and N. I. Zheludev, *Opt. Express* **19**, 23279–23285 (2011).

²⁰K. Kumar, H. G. Duan, R. S. Hegde, S. C. W. Koh, J. N. Wei, and J. K. W. Yang, *Nat. Nanotechnol.* **7**, 557–561 (2012).

²¹D. Kuzum, R. G. Jeyasingh, B. Lee, and H. S. Wong, *Nano Lett.* **12**, 2179–2186 (2012).